Current-Controlled Nanomagnetic Writing for Reconfigurable Magnonic Crystals

Jack C. Gartside[1,*,†], Son G. Jung[1,3,†], Seung Y. Yoo[1,†], Daan M. Arroo[2], Alex Vanstone[1], Troy Dion[1,3], Kilian D. Stenning[1], and Will R. Branford[1]

[1]Blackett Laboratory, Imperial College London, London SW7 2AZ, United Kingdom
[2]London Centre for Nanotechnology, University College London, London WC1H 0AH, United Kingdom
[*]Corresponding author e-mail: j.carter-gartside13@imperial.ac.uk
[†]These authors contributed equally
[3]Present address: Cavendish Laboratory, University of Cambridge, Cambridge, CB3 0HE, United Kingdom

Supplementary Information

Supplementary note 1 - Gating of magnon centre-mode in low-power domain gate case

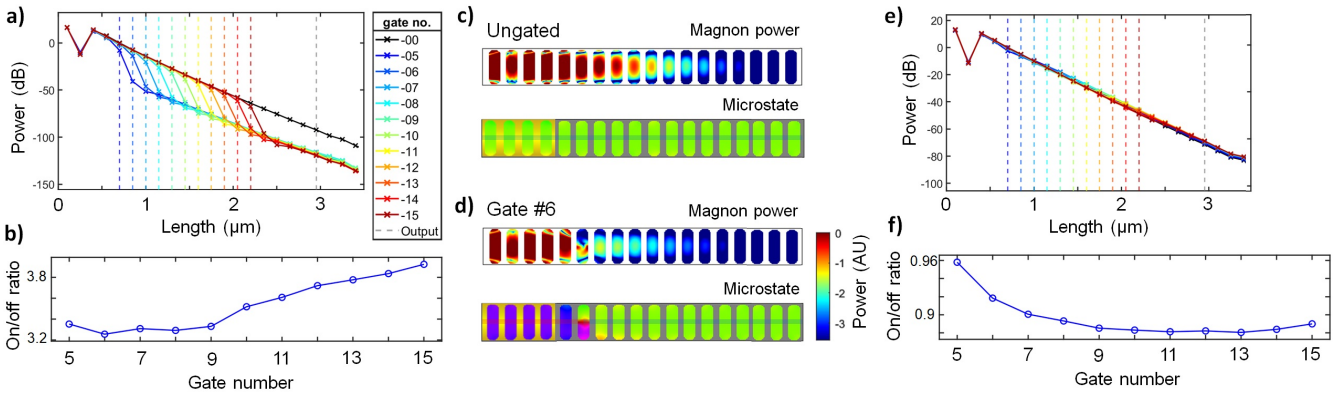

Supplementary figure 1. a) Bulk-mode spin-wave power vs. array position for 'domain' gate type with nanowire in low-power $h = 10$ nm mode. Coplanar microwave waveguide covers islands 1-4. Nanoisland positions denoted by dashed vertical lines with power vs. position traces colour-coded by gate position.
b) Corresponding magnon 'on/off' ratio vs. gate position, calculated from the ratio of integrated power at island 20 in the ungated to gated case.
c,d) Spatial power map and corresponding microstate of resonant magnon centre-mode for ungated (c) and gate position 6 (d) arrays in low-power mode. Power is normalised to ungated case. Array microstate is shown with green (purple) representing unswitched (switched) islands magnetised in the positive-y (negative-y) direction. Control nanowire is shown over array, coplanar Au waveguide covers islands 1-4. e,f) Bulk-mode spin-wave power vs. array position (a) and corresponding magnon 'on/off' ratio (b) for domain gate case simulated without suspended nanowire and c-DW. In the absence of the c-DW stray field there is no magnetisation distortion in the gate island, and hence very low magnon attenuation is observed.

So far the magnons considered have been edge-localised resonant modes. This is because nanoisland edges experience larger variation in local field (and hence larger variation in magnon response) than the centre of islands, as the local stray fields emanate from nanoisland ends. In the domain-gate case for the low-power, $h = 10$ nm mode the presence of the c-DW above the gate nanoisland induces significant vortex-like distortion of the island magnetisation, seen in fig. 1 d). This distortion is substantial at the nanoisland centre, and as such the centre-localised resonant magnon mode is more strongly attenuated in this gate case than other gate types discussed in this work. Fig. 1 e) and f) display the behaviour of the domain-gate simulated with no suspended nanowire and c-DW. In this case there is no magnetisation distortion in the gate-island and hence very low magnon attenuation is observed, demonstrating the utility of the c-DW method to locally distort magnetisation textures as well

as offer Ising-like reversal.

Supplementary note 2 - Additional microstates of the reconfigurable magnonic filter

The FM, AFM and stripe microstates considered so far have symmetrical island magnetisation arrangements, such that the same local dipolar stray field $\mathbf{H}_{\text{loc}}$ is felt at each island (relative to its magnetisation). This leads to a single well-defined magnon edge-mode ($\sim 1.5-3$ GHz) and centre-mode ($\sim 5-7$ GHz) for each microstate. However, the writing technique allows preparation of arbitrary microstates containing a range of $\mathbf{H}_{\text{loc}}$ profiles. Figure 2 shows a range of these 'mixed' microstates and their corresponding spectra. Figure 2 a) shows a mixed microstate constituting elements of the previously discussed FM/AFM/stripe states alongside spectra of those states. The mixed state exhibits overlapping modes corresponding to each of the microstates comprising it, resulting in a broader range of permitted magnon frequencies and an effective variable-bandwidth filtering mode.

Figure 2 b) shows the spectral effects of smoothly transitioning between microstates. The array is prepared in the stripe state and transitioned to the FM state via three interstitial mixed states, with one column of islands reversed between each microstate. The stripe mode smoothly decays away through the first three mixed states, becoming partially obscured from its overlap with the growing FM state from 'mixed 2' onwards before abruptly dropping once in the pure FM state. Similarly the FM state can be seen to grow from the mixed 2 state onwards once there are at least two adjacent columns of parallel-magnetised islands. Mixed states 2 and 3 contain aspects of the AFM microstate an as such a related mode at 1.5 GHz is observed. Much smoother microstate transitions are possible with larger unit-cell arrays than the four-column, six-row example used here.

Figure 2 c) shows five mixed microstates, each designed comprising aspects of the AFM, FM and stripe states with different relative aspects of each of the three microstates. Mixed states are ordered A)-E) by the relative amount of AFM microstate they contain, which is seen reflected in the AFM magnon mode intensities. Fine control of mode-amplitude tuning is achieved, with enhanced control of the relative mode intensities possible in larger arrays.

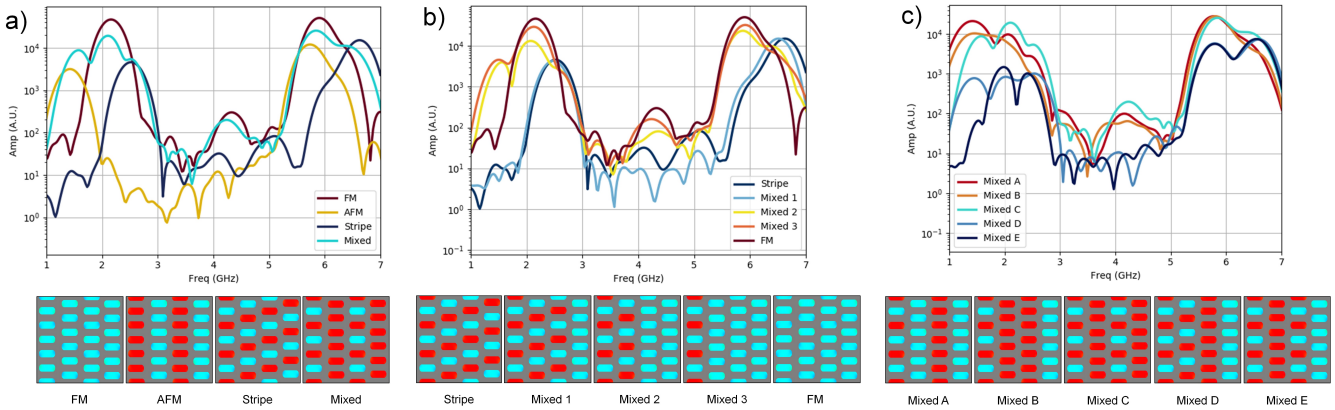

Supplementary figure 2. Spin-wave spectra of the two-dimensional RMC across a range of microstates. Microstates are shown underneath each spectra with red and blue islands denoting $M = +\hat{x}$ and $M = -\hat{x}$ respectively. A four-column, six-row unit cell is simulated with periodic boundary conditions in the x-direction.
a) Spectra of the FM, AFM, stripe and a 'mixed' microstate. Mixed microstate comprises elements of the three other states resulting in multiple edge and centre spin-wave modes, especially apparent in the $\sim 1-3$ GHz edge-mode region. These modes overlap, supporting a broader range of spin-wave frequencies in the RMC relative to the 'pure' microstates and an effective variable-bandwidth filtering mode.
b) Spectra showing gradual transition between stripe and FM microstates via three interstitial 'mixed' states, switching one column from stripe to FM between each mixed state.
Amplitude of the stripe mode is reduced and FM mode is increased as the transition progresses. AFM mode appears during the transition and is most prominent in 'mixed 2' state at the transition midpoint. Much smoother transitions with finer mode-amplitude control are possible with larger unit-cell arrays.
c) Spectra of five mixed states, showing the degree to which the relative amplitudes of the FM, AFM and stripe modes may be tuned via microstate design. 'Mixed C' state corresponds to the 'mixed' state from panel a). Microstates are named and ordered by the relative intensity of the ~ 1.5 GHz AFM mode. Again, much finer tuning of the relative mode intensities is possible with larger unit-cell arrays.